Journal of Solid State Chemistry **168,** 245–258 (2002)
doi:10.1006/jssc.2002.9717

Crystal Chemistry of Rubidium Uranyl Molybdates: Crystal Structures of $Rb_6[(UO_2)(MoO_4)_4]$, $Rb_6[(UO_2)_2O(MoO_4)_4]$, $Rb_2[(UO_2)(MoO_4)_2]$, $Rb_2[(UO_2)_2(MoO_4)_3]$ and $Rb_2[(UO_2)_6(MoO_4)_7(H_2O)_2]$

Sergey V. Krivovichev and[1] Peter C. Burns[2]

Department of Civil Engineering and Geological Sciences, University of Notre Dame, 156 Fitzpatrick Hall, Notre Dame, Indiana 46556-0767,

Received April 9, 2002; in revised form June 26, 2002; accepted July 16, 2002

Five Rb uranyl molybdates have been prepared by solid-state reactions and hydrothermal syntheses. The structure of each compound has been investigated using single-crystal X-ray diffraction data collected using Mo$K\alpha$ radiation and a Charge-Coupled-device-based area detector. The structure of $Rb_6[(UO_2)(MoO_4)_4]$ (monoclinic, $C2/c$, $Z = 4$, $a = 17.312(1)$ Å, $b = 11.5285(8)$ Å, $c = 13.916(1)$ Å, $\beta = 127.634(1)^\circ$, $V = 2199.4(3)$ Å^3, $R_1 = 0.029$) is based on finite clusters of composition $[(UO_2)(MoO_4)_4]^{6-}$ composed of a UrO_4 (Ur: UO_2^{2+} uranyl ion) tetragonal bipyramid that shares each equatorial vertex with an adjacent MoO_4 tetrahedron. The structure of $Rb_6[(UO_2)_2O(MoO_4)_4]$ (triclinic, $P\bar{1}$, $Z = 2$, $a = 10.1567(5)$ Å, $b = 10.1816(5)$ Å, $c = 13.1129(6)$ Å, $\alpha = 76.921(1)^\circ$, $\beta = 76.553(1)^\circ$, $\gamma = 65.243(1)^\circ$, $V = 1184.8(1)$ Å^3, $R_1 = 0.047$) is based upon chains of composition $[(UO_2)_2O(MoO_4)_4]^{6-}$ containing UrO_5 pentagonal bipyramids and MoO_4 tetrahedra. The structure of $Rb_2[(UO_2)(MoO_4)_2]$ (monoclinic, $P2_1/c$, $Z = 8$, $a = 12.302(1)$ Å, $b = 13.638(1)$ Å, $c = 13.508(1)$ Å, $\beta = 94.975(2)^\circ$, $V = 2257.8(4)$ Å^3, $R_1 = 0.059$) contains sheets of composition $[(UO_2)(MoO_4)_2]^{2-}$ involving corner-sharing UrO_5 pentagonal bipyramids and MoO_4 tetrahedra. The structure of $Rb_2[(UO_2)_2(MoO_4)_3]$ (orthorhombic, $Pna2_1$, $Z = 4$, $a = 20.214(1)$ Å, $b = 8.3744(4)$ Å, $c = 9.7464(5)$ Å, $V = 1649.9(1)$ Å^3, $R_1 = 0.027$) consists of a framework with composition $[(UO_2)_2(MoO_4)_3]^{2-}$ that involves corner-sharing UrO_5 pentagonal bipyramids and MoO_4 tetrahedra. The structure of $Rb_2[(UO_2)_6(MoO_4)_7(H_2O)_2]$ (orthorhombic, $Pbcm$, $Z = 4$, $a = 13.961(2)$ Å, $b = 10.7515(16)$ Å, $c = 25.579(4)$ Å, $V = 3839(1)$ Å^3, $R_1 = 0.037$) consists of a framework of corner-sharing UrO_5 pentagonal bipyramids, $UrO_4(H_2O)$ pentagonal bipyramids and MoO_4 tetrahedra. These structures are compared to those of other uranyl molybdates. The structural diversity and variability of uranyl molybdates is related to the high degree of flexibility of the U–O–Mo linkages. © 2002 Elsevier Science (USA)

Key Words: **rubidium uranyl molybdate; crystal structure; uranyl compounds.**

INTRODUCTION

Uranyl molybdates are important constituents of the oxidized zones of U–Mo deposits (1). They may also be significant in a geological repository for nuclear waste because ^{97}Mo is a fission product that forms during irradiation of nuclear fuel in a reactor. Recently, a Cs–Ba-bearing uranyl molybdate was found as an alteration-induced phase on spent nuclear fuel at 90°C in tests designed to simulate conditions expected in the proposed nuclear waste repository at Yucca Mountain, Nevada (2). Thus, uranyl molybdates may be important radionuclide-bearing phases during evolution of the repository.

Alkali metal uranyl molybdates have been extensively studied and several phases were described in the Na–U–Mo–O (3–7), K–U–Mo–O (8–11), and Cs–U–Mo–O (12–15) systems. However, until recently, structural studies have been done only for $K_2[(UO_2)(MoO_4)_2]$ (11). Recently, structures were determined for $Cs_2[(UO_2)(MoO_4)_2](H_2O)$ (15), $Rb_2[(UO_2)(MoO_4)_2](H_2O)$ (16), $K_2[(UO_2)(MoO_4)_2](H_2O)$ (17), $Na_2[(UO_2)(MoO_4)_2]$ (17), $Na_6[(UO_2)(MoO_4)_4]$ (18), $Na_6[(UO_2)_2O(MoO_4)_4]$ (18), $K_6[(UO_2)_2O(MoO_4)_4]$ (18), $Cs_6[(UO_2)(MoO_4)_4]$ (19), $Cs_4[(UO_2)_3Mo_3O_{14}]$ (19), $Cs_2(UO_2)_6(MoO_4)_7(H_2O)_2$ (20), and α- and β-$Cs_2[(UO_2)_2(MoO_4)_3]$ (21). Although the structures of many compounds in the Na–U–Mo–O, K–U–Mo–O and Cs–U–Mo–O systems are now known, little is known concerning Rb uranyl molybdates. The only structure reported to date is that of $Rb_2[(UO_2)(MoO_4)_2](H_2O)$ (16). The anhydrous analogue, $Rb_2[(UO_2)(MoO_4)_2]$, was studied by Tatarinova

[1] Permanent address: Department of Crystallography, St. Petersburg State University, University Emb. 7/9, 199034 St. Petersburg, Russia.

[2] To whom correspondence should be addressed. Fax: +219-631-9236. E-mail: pburns@nd.edu.

0022-4596/02 $35.00

TABLE 1
Crystallographic Data and Refinement Parameters for Rubidium Uranyl Molybdates

Compound	$Rb_6[(UO_2)(MoO_4)_4]$	$Rb_6[(UO_2)_2O(MoO_4)_4]$	$Rb_2[(UO_2)(MoO_4)_2]$	$Rb_2[(UO_2)_2(MoO_4)_3]$	$Rb_2[(UO_2)_6(MoO_4)_7(H_2O)_2]$
Color	Pale yellow	Orange	Lemon yellow	Yellow	Light yellow
Crystal habit	Plates	Isometric	(001) plates	Isometric	Needles
a (Å)	17.312(1)	10.1567(5)	12.302(1)	20.214(1)	13.961(2)
b (Å)	11.5285(8)	10.1816(5)	13.638(1)	8.3744(4)	10.752(2)
c (Å)	13.916(1)	13.1129(6)	13.508(1)	9.7464(5)	25.579(4)
α (deg)	—	76.921(1)	—	—	—
β (deg)	127.634(1)	76.553(1)	94.975(2)	—	—
γ (deg)	—	65.243(1)	—	—	—
V (Å^3)	2199.4(3)	1184.8(1)	2257.8(4)	1649.9(1)	3839(1)
Space group	$C2/c$	$P\bar{1}$	$P2_1/c$	$Pna2_1$	$Pbcm$
Ref. for cell refinement	2759	4828	2725	6234	1606
F_{000}	2504	1484	2640	2048	5040
$\phi\mu/\phi$ (cm^{-1})	228.22	280.02	250.95	277.16	300.43
Z	4	2	8	4	4
D_{calc} (g/cm^3)	4.30	4.79	4.48	4.79	5.10
Crystal size (mm^3)	$0.14 \times 0.12 \times 0.10$	$0.38 \times 0.28 \times 0.18$	$0.09 \times 0.08 \times 0.02$	$0.18 \times 0.12 \times 0.08$	$0.18 \times 0.02 \times 0.01$
Radiation	Mo$K\alpha$	Mo$K\alpha$	Mo$K\alpha$	Mo$K\alpha$	Mo$K\alpha$
Absorption correction	Ellipsoid	Ellipsoid	Ellipsoid	Ellipsoid	Ellipsoid
Ref. for absorption corr.	1572	2240	1316	3679	712
R_{int}	13.5→4.4%	18.9→6.0%	10.1→5.3%	17.3→5.6%	8.9→5.5%
Total ref.	12 117	13 283	24 666	17 739	41 489
Unique ref.	4526	9277	9051	6139	8150
Unique $\lvert F_o\rvert \geq 4\sigma_F$	3211	7090	5171	5385	3747
R_1	0.029	0.047	0.059	0.027	0.037
wR_2	0.047	0.105	0.131	0.045	0.073
S	0.739	1.007	0.906	0.807	0.748

Note. $R_1 = \sum ||F_o| - |F_c|| / \sum |F_o|$; $wR_2 = \sum [w(F_o^2 - F_c^2)^2] / \sum [wF_o^2)^2]^{1/2}$; $w = 1/[\sigma^2(F_o^2) + (aP)^2 + bP]$, where $P = (F_o^2 + 2F_c^2)/3$; $s = \sum [w(F_o^2 - F_c^2)]/(n-p)^{1/2}$ where n is the number of reflections and p is the number of refined parameters.

et al. (22), who determined its space group and unit-cell parameters, but not its entire structure.

The purpose of the current study is to report syntheses and crystal-structure determinations of five Rb uranyl molybdates and to compare them with similar structures of Na, K, and Cs uranyl molybdates.

EXPERIMENTAL

Syntheses of Crystals of Rb Uranyl Molybdates

Synthesis conditions for each phase were selected on the basis of our previous studies of uranyl molybdates (17–21). Crystals of $Rb_6[(UO_2)(MoO_4)_4]$, $Rb_6[(UO_2)_2O(MoO_4)_4]$, $Rb_2[(UO_2)(MoO_4)_2]$, and $Rb_2[(UO_2)_2(MoO_4)_3]$ used in this study were obtained by high-temperature solid-state reaction in platinum crucibles at 700°C in air, followed by cooling to 300°C over 100 h and then to 50°C over 10 h.

$Rb_6[(UO_2)(MoO_4)_4]$. The reactants were $RbNO_3$ (0.0888 g, Alfa Aesar, 99%), UO_3 (0.0286 g, Alfa Aesar, 99.8%), and MoO_3 (0.0576 g, Sigma, 99.5%) powders. The product consisted of pale-yellow platy to isometric crystals up to 0.5 mm in maximum length.

$Rb_6[(UO_2)_2O(MoO_4)_4]$. The reactants were $RbNO_3$ (0.0592 g), UO_3 (0.0286 g) and MoO_3 (0.0432 g) powders. The product consisted of orange transparent isometric crystals of $Rb_6[(UO_2)_2O(MoO_4)_4]$ and lemon-yellow plates of $Rb_2[(UO_2)(MoO_4)_2]$.

$Rb_2[(UO_2)(MoO_4)_2]$. The reactants were $RbNO_3$ (0.0592 g), UO_3 (0.0858 g), and MoO_3 (0.0720 g) powders. The product consisted of lemon-yellow plates of $Rb_2[(UO_2)(MoO_4)_2]$ and dark-yellow isometric crystals of $Rb_2[(UO_2)_2(MoO_4)_3]$.

$Rb_2[(UO_2)_2(MoO_4)_3]$. The reactants were $RbNO_3$ (0.0592 g), UO_3 (0.0858 g), and MoO_3 (0.0720 g) powders. The product consisted of dark-yellow isometric crystals of $Rb_2[(UO_2)_2(MoO_4)_3]$.

Crystals of $Rb_2[(UO_2)_6(MoO_4)_7(H_2O)_2]$ were obtained by hydrothermal methods. They were grown from a solution of $RbNO_3$, $UO_2(CH_3COO)_2 \cdot 2H_2O$ (Alfa Aesar, 98%) and MoO_3 (0.0148, 0.0392 and 0.0144 g, respectively) in 5 mL of H_2O. The solution was placed in a 23 mL

TABLE 2
Atomic Coordinates and Displacement Parameters ($\times 10^4$ Å^2) for $Rb_6[(UO_2)(MoO_4)_4]$

	x	y	z	U_{eq}	U_{11}	U_{22}	U_{33}	U_{23}	U_{13}	U_{12}
U(1)	0	$\frac{1}{2}$	0	124(1)	119(1)	118(1)	136(1)	7(1)	78(1)	8(1)
Mo(1)	0.06283(3)	0.81323(3)	0.04424(3)	162(1)	172(2)	132(2)	182(2)	−7(1)	108(2)	−14(1)
Mo(2)	0.23756(3)	0.44069(3)	0.07074(3)	167(1)	125(2)	136(2)	235(2)	−18(1)	107(2)	−3(1)
Rb(1)	0	0.31556(5)	$-\frac{1}{4}$	205(1)	192(3)	188(3)	239(3)	0	133(3)	0
Rb(2)	0	0.99038(5)	$-\frac{1}{4}$	200(1)	200(3)	164(3)	244(3)	0	140(2)	0
Rb(3)	0.35757(3)	0.82355(4)	0.16320(4)	269(1)	236(2)	203(2)	293(2)	13(2)	122(2)	−16(2)
Rb(4)	0.28674(3)	0.36138(4)	−0.16717(4)	259(1)	226(2)	297(2)	258(2)	−3(2)	150(2)	3(2)
O(1)	−0.0017(2)	0.4608(2)	0.1239(3)	202(7)	250(17)	165(14)	227(16)	16(12)	165(14)	−12(13)
O(2)	0.0807(2)	0.6640(2)	0.1007(2)	185(7)	202(16)	120(14)	174(14)	19(11)	85(13)	−11(12)
O(3)	0.1440(2)	0.4054(3)	0.0896(3)	226(7)	148(16)	228(16)	291(16)	72(13)	128(14)	12(13)
O(4)	0.1848(2)	0.4378(3)	−0.0834(3)	260(7)	208(17)	295(18)	242(16)	−46(14)	118(14)	−32(15)
O(5)	−0.0154(2)	0.8832(3)	0.0639(3)	309(8)	268(19)	320(19)	313(18)	−54(15)	164(16)	77(15)
O(6)	0.0078(3)	0.8047(3)	−0.1105(3)	309(8)	51(2)	186(15)	222(16)	34(13)	215(16)	−27(16)
O(7)	0.3321(2)	0.3405(3)	0.1470(3)	295(8)	167(17)	267(17)	420(20)	60(15)	159(15)	54(14)
O(8)	0.2844(2)	0.5807(3)	0.1239(3)	285(8)	307(19)	217(17)	370(19)	−69(15)	227(16)	−72(15)
O(9)	0.1751(2)	0.8822(3)	0.1219(3)	335(8)	252(19)	272(18)	480(20)	−60(16)	227(17)	−125(15)

Teflon-lined Parr vessel and heated to 230°C for 24 h, followed by cooling to ambient temperature. The crystals occur as aggregates of transparent yellow needles up to 0.2 mm in maximum length.

X-Ray Diffraction Data Collection

The crystals selected for data collection were mounted on a Bruker three-circle diffractometer equipped with a

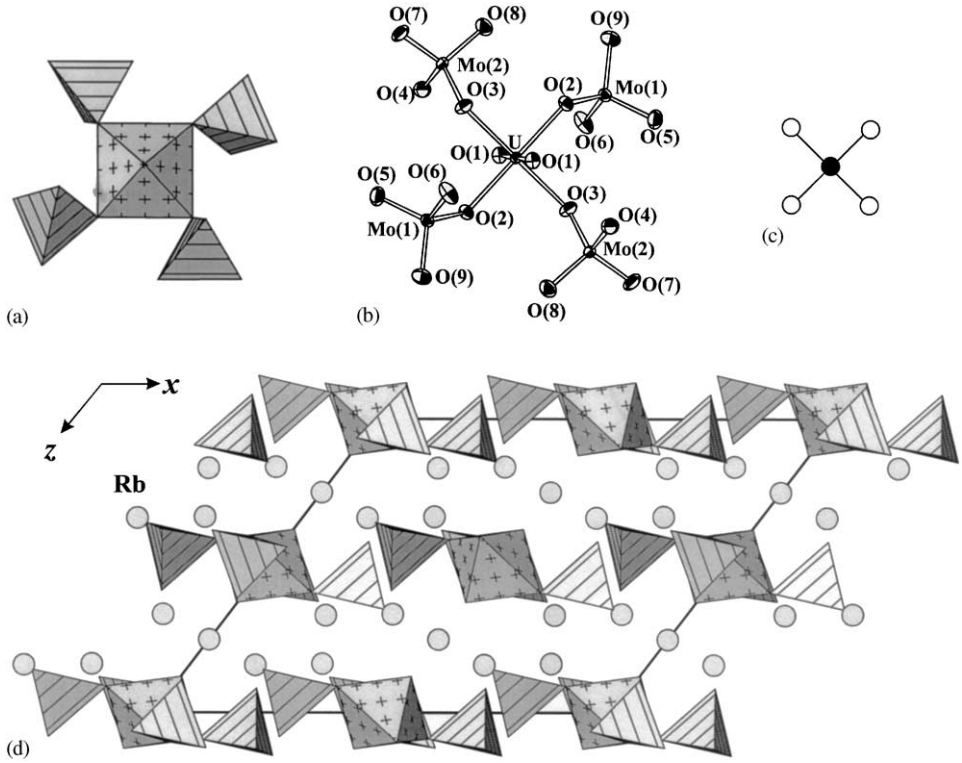

FIG. 1. The $[(UO_2)(MoO_4)_4]^{6-}$ cluster in the structure of $Rb_6[(UO_2)(MoO_4)_4]$ shown in polyhedral representation (a), ball-and-stick representation (b) (ellipsoids are drawn at the 50% probability level), and nodal representation (c) (insets: U = black, Mo = white). (d) Projection of the structure of $Rb_6[(UO_2)(MoO_4)_4]$ along [010]. Uranyl and molybdate polyhedra are shaded with crosses and parallel lines, respectively.

TABLE 3
Selected Bond Lengths (Å) in the Structure of $Rb_6[(UO_2)(MoO_4)_4]$

U(1)–O(1),*a*	1.800(3) 2 ×	Rb(2)–O(6),*b*	2.837(3) 2 ×
U(1)–O(2),*a*	2.258(3) 2 ×	Rb(2)–O(5)*f*,*g*	2.839(3) 2 ×
U(1)–O(3),*a*	2.273(3) 2 ×	Rb(2)–O(7)*h*,*i*	3.036(3) 2 ×
⟨U(1)–O_{Ur}⟩	1.80	Rb(2)–O(8)*h*,*i*	3.112(3) 2 ×
⟨U(1)–O_{eq}⟩	2.27	⟨Rb(2)–O⟩	2.96
Mo(1)–O(5)	1.735(3)	Rb(3)–O(4)*i*	2.889(3)
Mo(1)–O(9)	1.736(3)	Rb(3)–O(1)*j*	2.912(3)
Mo(1)–O(6)	1.746(3)	Rb(3)–O(9)	2.924(4)
Mo(1)–O(2)	1.837(3)	Rb(3)–O(6)*k*	2.977(3)
⟨Mo(1)–O⟩	1.76	Rb(3)–O(8)	2.983(3)
		Rb(3)–O(6)*i*	3.200(4)
Mo(2)–O(7)	1.737(3)	Rb(3)–O(1)*l*	3.220(3)
Mo(2)–O(4)	1.745(3)	Rb(3)–O(8)*i*	3.351(3)
Mo(2)–O(8)	1.754(3)	⟨Rb(3)–O⟩	3.06
Mo(2)–O(3)	1.837(3)		
⟨Mo(2)–O⟩	1.77	Rb(4)–O(4)	2.786(3)
		Rb(4)–O(5)*m*	2.947(3)
Rb(1)–O(4),*b*	2.922(3) 2 ×	Rb(4)–O(8)*e*	2.959(3)
Rb(1)–O(7)*c*,*d*	2.942(3) 2 ×	Rb(4)–O(9)*i*	3.011(3)
Rb(1)–O(1)*a*,*e*	3.108(3) 2 ×	Rb(4)–O(2)*e*	3.029(3)
Rb(1)–O(2)*a*,*e*	3.141(3) 2 ×	Rb(4)–O(7)*d*	3.229(3)
Rb(1)–O(5)*a*,*e*	3.344(4) 2 ×	Rb(4)–O(3)*d*	3.237(3)
⟨Rb(1)–O⟩	3.09	Rb(4)–O(6)*m*	3.465(4)
		⟨Rb(4)–O⟩	3.08

Note. $a = -x, -y+1, -z$; $b = -x, y, -z+\frac{1}{2}$; $c = x-\frac{1}{2}, -y+\frac{1}{2}, z-\frac{1}{2}$; $d = -x+\frac{1}{2}, -y+\frac{1}{2}, -z$; $e = x, -y+1, z-\frac{1}{2}$; $f = -x, -y+2, -z$; $g = x, -y+2, z-\frac{1}{2}$; $h = x-\frac{1}{2}, -y+\frac{3}{2}, z-\frac{1}{2}$; $i = -x+\frac{1}{2}, -y+\frac{3}{2}, -z$; $j = -x+\frac{1}{2}, y+\frac{1}{2}, -z+\frac{1}{2}$; $k = x+\frac{1}{2}, -y+\frac{3}{2}, z+\frac{1}{2}$; $l = x+\frac{1}{2}, y+\frac{1}{2}, z$; $m = x+\frac{1}{2}, y-\frac{1}{2}, z$.

SMART APEX charge-coupled device (CCD) detector with a crystal-to-detector distance of 5 cm. The data were collected using monochromated Mo$K\alpha$ X-ray radiation and frame widths of 0.3° in ω. The unit-cell dimensions (Table 1) were refined using least-squares techniques. More than a hemisphere of data was collected for each crystal and the three-dimensional data sets were reduced and filtered for statistical outliers using the Bruker program SAINT. The data were corrected for Lorentz, polarization and background effects. Semi-empirical absorption corrections were done by modeling all the crystals as ellipsoids using the Bruker program XPREP. Additional information pertinent to the data collections is given in Table 1.

Structure Solution and Refinement

Scattering curves for neutral atoms, together with anomalous-dispersion corrections, were taken from International Tables for X-ray Crystallography, Vol. IV (23). The Bruker SHELXTL Version 5 system of programs was used for the determination and refinement of the structure. The structures of $Rb_6[(UO_2)(MoO_4)_4]$ and $Rb_6[(UO_2)_2O(MoO_4)_4]$ were solved by direct methods and refined to $R_1 = 2.9\%$ and 4.7%, respectively. The structures of $Rb_2[(UO_2)(MoO_4)_2]$, $Rb_2[(UO_2)_2(MoO_4)_3]$, and $Rb_2[(UO_2)_6(MoO_4)_7(H_2O)_2]$ were refined on the basis of atomic coordinates for $K_2[(UO_2)(MoO_4)_2]$ (11), $Cs_2[(UO_2)_2(MoO_4)_3]$ (21), and $Cs_2[(UO_2)_6(MoO_4)_7(H_2O)_2]$ (20), respectively, and gave $R_1 = 5.9\%, 2.7\%$, and 3.7%,

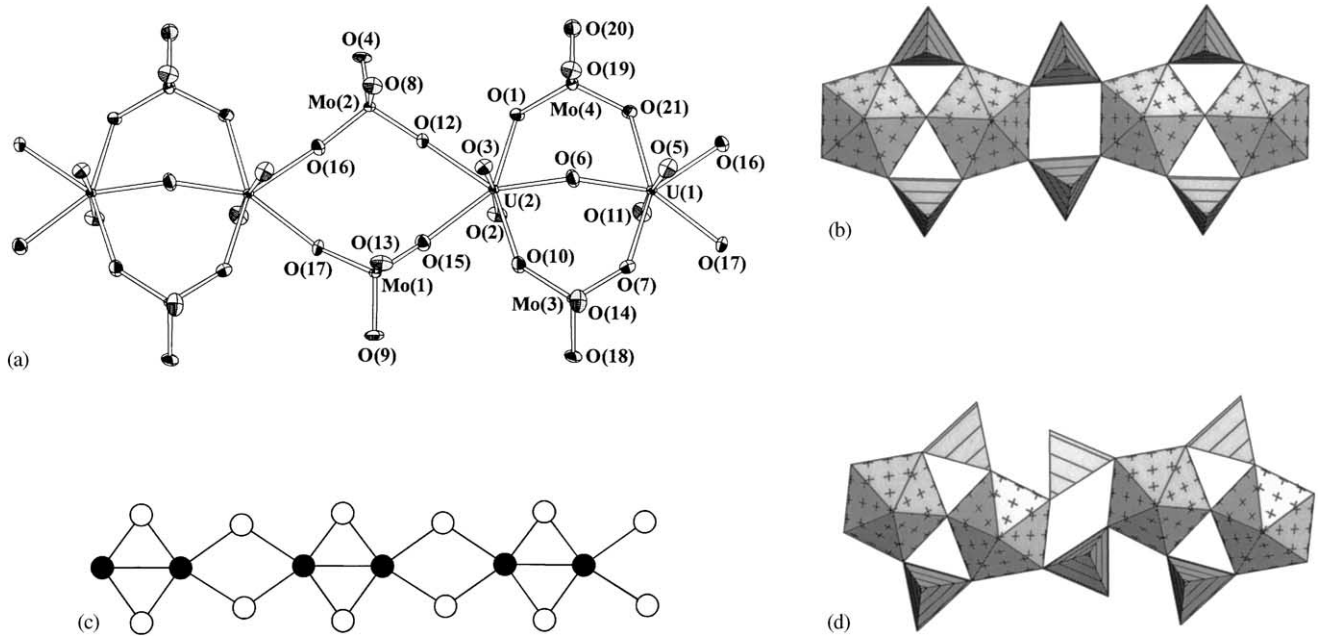

FIG. 2. The $[(UO_2)_2O(MoO_4)_4]^{6-}$ chain in the structure of $Rb_6[(UO_2)_2O(MoO_4)_4]$. (a) ball-and-stick representation (ellipsoids are drawn at the 50% probability level), (b) polyhedral representation, (c) nodal representation (insets: U = black, Mo = white). (d) The $[(UO_2)_2O(MoO_4)_4]^{6-}$ chain in the structure of $Na_6[(UO_2)_2O(MoO_4)_4]$. Legend as in Fig. 1.

TABLE 4
Atomic Coordinates and Displacement Parameters ($\times 10^4$ Å^2) for $Rb_6[(UO_2)_2O(MoO_4)_4]$

	x	y	z	U_{eq}	U_{11}	U_{22}	U_{33}	U_{23}	U_{13}	U_{12}
U(1)	0.91347(3)	0.05739(3)	0.23023(2)	82(1)	98(1)	79(1)	69(1)	−19(1)	6(1)	−39(1)
U(2)	0.29822(3)	0.66259(3)	0.23153(2)	78(1)	90(1)	91(13)	51(1)	−13(1)	−2(1)	−37(1)
Mo(1)	0.74134(8)	0.50053(7)	0.12359(5)	98(1)	108(3)	100(3)	82(3)	−7(2)	11(2)	−51(2)
Mo(2)	0.48092(8)	0.23664(7)	0.36338(6)	95(1)	110(3)	101(3)	81(3)	−11(2)	−6(2)	−52(2)
Mo(3)	0.30779(8)	0.04307(7)	0.09647(6)	107(1)	122(3)	103(3)	91(3)	−9(2)	16(3)	−58(2)
Mo(4)	−0.04800(8)	0.71438(8)	0.40326(6)	128(1)	134(3)	117(3)	136(3)	−42(2)	−15(3)	−42(3)
Rb(1)	−0.20145(11)	0.05057(10)	0.56150(7)	206(2)	213(5)	213(4)	191(4)	−50(3)	−2(4)	−−85(3)
Rb(2)	0.03186(10)	0.27784(10)	−0.07166(7)	184(2)	169(4)	195(4)	202(4)	−44(3)	−22(3)	−80(3)
Rb(3)	0.54785(13)	0.27763(12)	0.07027(7)	280(2)	421(6)	409(6)	90(4)	−16(4)	6(4)	−273(5)
Rb(4)	0.58628(11)	−0.13894(11)	0.28436(9)	262(2)	217(5)	242(5)	326(5)	−90(4)	-62(4)	−53(4)
Rb(5)	0.11418(12)	0.33709(11)	0.27391(10)	285(2)	250(5)	200(4)	435(6)	−124(4)	−27(5)	−91(4)
Rb(6)	0.70056(12)	0.45092(11)	0.43526(8)	253(2)	336(6)	316(5)	159(4)	2(4)	−8(4)	−211(4)
O(1)	0.1007(8)	0.5962(6)	0.3203(5)	175(13)	240(40)	110(30)	150(30)	−70(20)	70(30)	−80(30)
O(2)	0.2501(8)	0.6478(8)	0.1133(5)	193(13)	210(30)	310(40)	130(30)	−40(30)	−60(30)	−150(30)
O(3)	0.3689(8)	0.6661(7)	0.3466(5)	177(13)	270(40)	200(30)	100(30)	−40(20)	−60(30)	−100(30)
O(4)	0.3860(8)	0.1206(7)	0.4011(5)	191(14)	230(40)	220(30)	170(30)	−20(30)	50(30)	−180(30)
O(5)	0.9203(8)	0.1266(7)	0.3450(5)	219(15)	310(40)	260(30)	150(30)	−50(30)	−130(30)	−100(30)
O(6)	0.1081(7)	0.8591(7)	0.2685(6)	223(14)	130(30)	170(30)	330(40)	−60(30)	10(30)	−40(30)
O(7)	0.1118(8)	0.1223(7)	0.1333(6)	216(14)	210(40)	170(30)	230(40)	20(30)	0(30)	−80(30)
O(8)	0.5204(8)	0.2734(8)	0.4747(5)	214(14)	270(40)	280(40)	150(30)	−80(30)	−40(30)	−140(30)
O(9)	0.8103(8)	0.5660(7)	−0.0019(5)	209(14)	280(40)	220(30)	140(30)	0(20)	40(30)	−160(30)
O(10)	0.3750(8)	−0.1511(7)	0.1367(6)	256(16)	140(30)	150(30)	440(50)	−30(30)	50(30)	−70(30)
O(11)	0.8915(8)	0.0052(8)	0.1168(6)	241(15)	270(40)	280(40)	220(40)	−110(30)	−30(30)	−120(30)
O(12)	0.3787(7)	0.4004(7)	0.2862(5)	190(13)	140(30)	120(30)	230(30)	−10(20)	10(3)	−20(20)
O(13)	0.7898(8)	0.5619(8)	0.2193(5)	238(15)	340(40)	360(40)	100(30)	−70(30)	−20(3)	−210(30)
O(14)	0.3760(8)	0.1161(8)	0.1709(6)	267(17)	300(40)	250(40)	260(40)	−140(30)	−100(3)	−40(30)
O(15)	0.5470(7)	0.5549(7)	0.1408(6)	200(14)	160(30)	190(30)	250(40)	−50(30)	−20(3)	−70(30)
O(16)	0.6489(7)	0.1509(7)	0.2808(5)	209(14)	130(30)	220(30)	210(30)	−10(30)	−20(3)	−20(30)
O(17)	0.8209(8)	0.3064(7)	0.1423(6)	223(15)	180(30)	100(30)	290(40)	10(30)	0(3)	0(20)
O(18)	0.3478(8)	0.0889(8)	−0.0403(5)	236(15)	220(40)	290(40)	090(30)	20(30)	30(3)	−60(30)
O(19)	0.0126(8)	0.7523(8)	0.5021(6)	240(15)	290(40)	300(40)	210(40)	−90(30)	−30(3)	−160(30)
O(20)	−0.1574(8)	0.6194(7)	0.4628(6)	253(16)	220(40)	210(30)	330(40)	−30(30)	−20(3)	−100(30)
O(21)	−0.1689(7)	0.8791(7)	0.3353(6)	262(16)	100(30)	220(30)	380(40)	90(30)	20(3)	−80(30)

respectively. For all structures except $Rb_2[(UO_2)(MoO_4)_2]$, final models include anisotropic displacement parameters of all atoms. For $Rb_2[(UO_2)(MoO_4)_2]$, a model that included anisotropic displacement parameters for the anions was tried but resulted in non-positive-definite parameters for O atoms belonging to the uranyl ions. Consequently, we refined these atoms isotropically. This situation is common when refining the structures of uranyl compounds owing to the large difference in the atomic scattering factors for uranium and oxygen. In the case of $Rb_2[(UO_2)_6(MoO_4)_7(H_2O)_2]$, the isotropic displacement parameter for the Rb(2) site is unusually large. This may indicate positional disorder, which is frequently observed for low-valence cation positions in framework cavities. Our data do not support splitting the Rb(2) site. The final atomic positional and displacement parameters, and selected interatomic distances for $Rb_6[(UO_2)(MoO_4)_4]$ are in Tables 2 and 3, respectively, for $Rb_6[(UO_2)_2O(MoO_4)_4]$ are in Tables 4 and 5, respectively, for $Rb_2[(UO_2)(MoO_4)_2]$ are in Tables 6 and 7, respectively, for $Rb_2[(UO_2)_2(MoO_4)_3]$ are in Tables 8 and 9, respectively, for $Rb_2[(UO_2)_6(MoO_4)_7(H_2O)_2]$ are in Tables 10 and 11, respectively. Tables of observed and calculated structure factors are available from the authors upon request.

RESULTS

Cation Coordination Polyhedra

Uranium. In each of the structures reported in this study, U^{6+} cations are part of approximately linear $(UO_2)^{2+}$ uranyl ions (designated *Ur*), as is almost invariably observed in uranyl compounds (24–26). In the structure of $Rb_6[(UO_2)(MoO_4)_4]$, the uranyl ions are coordinated by four O atoms arranged at the equatorial corners of tetragonal bipyramids that are capped by O_{Ur} atoms. In the structures of $Rb_6[(UO_2)_2O(MoO_4)_4]$, $Rb_2[(UO_2)(MoO_4)_2]$, and $Rb_2[(UO_2)_2(MoO_4)_3]$, the uranyl

TABLE 5
Selected Bond Lengths (Å) in the Structure of $Rb_6[(UO_2)_2O(MoO_4)_4]$

U(1)–O(11)	1.777(7)	Mo(4)–O(20)	1.713(7)	Rb(4)–O(21)*a*	2.806(7)
U(1)–O(5)	1.827(6)	Mo(4)–O(19)	1.733(7)	Rb(4)–O(14)	2.932(7)
U(1)–O(6)*a*	2.213(7)	Mo(4)–O(1)	1.794(6)	Rb(4)–O(4)	3.056(7)
U(1)–O(21)*a*	2.344(7)	Mo(4)–O(21)	1.796(7)	Rb(4)–O(13)*h*	3.059(7)
U(1)–O(7)*b*	2.378(7)	⟨Mo(4)–O⟩	1.76	Rb(4)–O(18)*j*	3.082(7)
U(1)–O(17)	2.413(6)			Rb(4)–O(16)	3.258(7)
U(1)–O(16)	2.425(7)	Rb(1)–O(5)*d*	2.891(7)	Rb(4)–O(10)	3.260(8)
⟨U(1)–O_{Ur}⟩	1.80	Rb(1)–O(4)*e*	2.951(6)	Rb(4)–O(8)*g*	3.275(7)
⟨U(1)–O_{eq}⟩	2.35	Rb(1)–O(3)*f*	3.030(6)	Rb(4)–O(3)*h*	3.403(7)
		Rb(1)–O(5)*g*	3.037(7)	⟨Rb(4)–O⟩	3.13
U(2)–O(2)	1.784(6)	Rb(1)–O(19)*h*	3.051(7)		
U(2)–O(3)	1.829(6)	Rb(1)–O(6)*f*	3.059(7)	Rb(5)–O(1)	2.780(6)
U(2)–O(6)	2.176(6)	Rb(1)–O(8)*d*	3.063(7)	Rb(5)–O(14)	2.942(7)
U(2)–O(10)*c*	2.340(7)	Rb(1)–O(19)*f*	3.182(7)	Rb(5)–O(19)*f*	3.021(7)
U(2)–O(1)	2.352(7)	⟨Rb(1)–O⟩	3.03	Rb(5)–O(12)	3.059(7)
U(2)–O(15)	2.423(7)			Rb(5)–O(7)	3.174(7)
U(2)–O(12)	2.427(6)	Rb(2)–O(2)*i*	2.793(7)	Rb(5)–O(4)	3.262(7)
⟨U(2)–O_{Ur}⟩	1.81	Rb(2)–O(11)*j*	2.818(7)	Rb(5)–O(13)*d*	3.263(8)
⟨U(2)–O_{eq}⟩	2.34	Rb(2)–O(7)	2.899(7)	Rb(5)–O(5)*d*	3.334(7)
		Rb(2)–O(13)*k*	3.017(7)	Rb(5)–O(9)*k*	3.472(7)
Mo(1)–O(9)	1.732(6)	Rb(2)–O(9)*d*	3.039(7)	⟨Rb(5)–O⟩	3.15
Mo(1)–O(13)	1.763(6)	Rb(2)–O(18)	3.042(7)		
Mo(1)–O(17)	1.777(6)	Rb(2)–O(9)*k*	3.094(7)	Rb(6)–O(20)*b*	2.784(7)
Mo(1)–O(15)	1.786(7)	Rb(2)–O(17)*d*	3.098(7)	Rb(6)–O(3)*l*	2.884(6)
⟨Mo(1)–O⟩	1.76	⟨Rb(2)–O⟩	2.98	Rb(6)–O(13)	2.887(7)
				Rb(6)–O(19)*l*	2.956(8)
Mo(2)–O(4)	1.743(6)	Rb(3)–O(14)	2.801(8)	Rb(6)–O(8)	2.965(7)
Mo(2)–O(8)	1.753(6)	Rb(3)–O(2)*k*	2.960(7)	Rb(6)–O(8)*l*	3.050(7)
Mo(2)–O(12)	1.776(6)	Rb(3)–O(16)	2.990(7)	Rb(6)–O(5)	3.414(7)
Mo(2)–O(16)	1.780(7)	Rb(3)–O(15)*k*	3.038(7)	Rb(6)–O(3)	3.462(7)
⟨Mo(2)–O⟩	1.76	Rb(3)–O(10)*j*	3.064(8)	⟨Rb(6)–O⟩	3.05
		Rb(3)–O(15)	3.159(6)		
Mo(3)–O(18)	1.744(6)	Rb(3)–O(12)	3.174(7)		
Mo(3)–O(14)	1.750(7)	Rb(3)–O(17)	3.270(7)		
Mo(3)–O(10)	1.794(7)	⟨Rb(3)–O⟩	3.06		
Mo(3)–O(7)	1.797(7)				
⟨Mo(3)–O⟩	1.77				

Note. $a = x+1, y-1, z$; $b = x+1, y, z$; $c = x, y+1, z$; $d = x-1, y, z$; $e = -x, -y, -z+1$; $f = -x, -y+1, -z+1$; $g = -x+1, -y, -z+1$; $h = x, y-1, z$; $i = -x, -y+1, -z$; $j = -x+1, -y, -z$; $k = -x+1, -y+1, -z$; $l = -x+1, -y+1, -z+1$.

ions are coordinated by five O atoms arranged at the equatorial corners of pentagonal bipyramids. In the structure of $Rb_2[(UO_2)_6(MoO_4)_7(H_2O)_2]$, there are four symmetrically independent uranyl ions. The $(U(1)O_2)^{2+}$ and $(U(4)O_2)^{2+}$ ions are coordinated by four O atoms and H_2O groups each, giving tetragonal bipyramids, whereas the $(U(2)O_2)^{2+}$ and $(U(3)O_2)^{2+}$ ions are coordinated by five O atoms each, giving pentagonal bipyramids.

Molybdenium. Mo^{6+} cations are tetrahedrally coordinated by four O atoms in each of the Rb uranyl molybdates studied. The ⟨Mo–O⟩ bond length in the MoO_4 tetrahedra varies from 1.75 to 1.78 Å, which is typical for uranyl molybdates (17–21).

Rubidium. In the structures under consideration, Rb^+ cations are coordinated by from eight to 12 ligands (O atoms and H_2O groups) with ⟨Rb–ϕ⟩ (ϕ: O, H_2O) bond lengths ranging from 2.96 to 3.25 Å.

Bond–Valence Analyses

The bond–valence sums for the atoms in each structure were calculated using parameters given by Burns *et al.* (26) for U^{6+}–O bonds and by Brese and O'Keeffe (27) for Mo^{6+}–O and Rb^+–O bonds. The results are summarized in Table 12. Bond valence sums for the Rb atoms range from 0.78 to 1.28 valence units (v.u.), those for the U atoms range from 5.62 to 6.43 v.u., those for the Mo atoms range

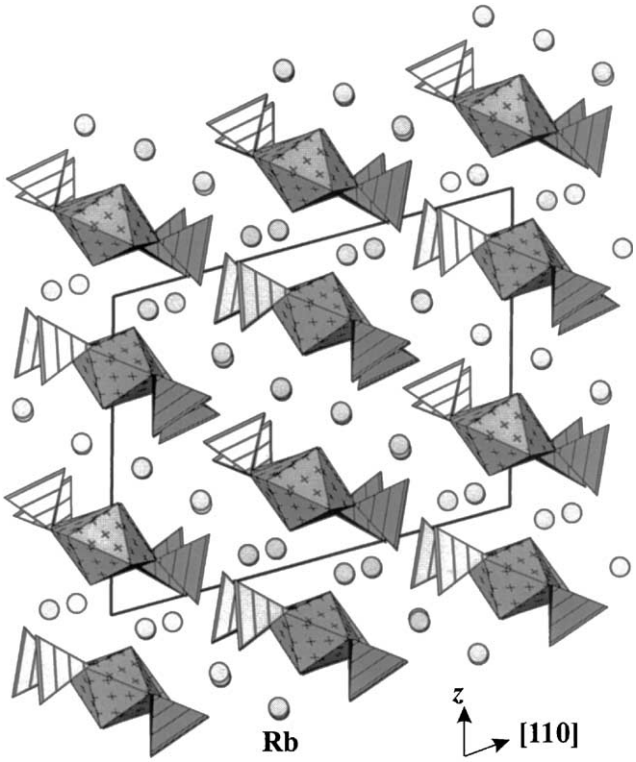

FIG. 3. Polyhedral representation of the structure of $Rb_6[(UO_2)_2O(MoO_4)_4]$ projected onto the $(\bar{1}10)$ plane. Legend as in Fig. 1.

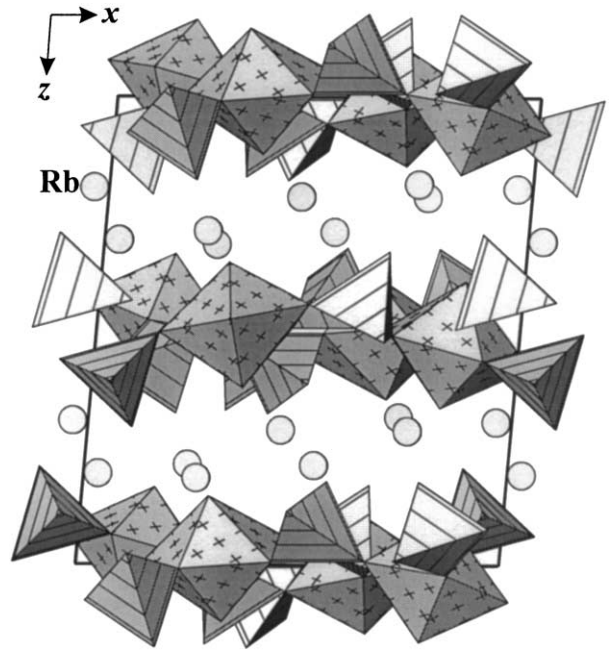

FIG. 5. Polyhedral representation of the structure of $Rb_2[(UO_2)(MoO_4)_2]$ projected along [010]. Legend as in Fig. 1.

from 5.79 to 6.13 v.u., and those for the O atoms range from 1.61–2.23 v.u. The bond-valence sums at the H_2O positions in the structure of $Rb_2[(UO_2)_6(MoO_4)_7(H_2O)_2]$ are in the range 0.51 to 0.61 v.u., which is in agreement with their assignment as water groups.

Structure Descriptions

$Rb_6[(UO_2)(MoO_4)_4]$. The structure is based on a cluster with composition $[(UO_2)(MoO_4)_4]^{6-}$ that involves a *Ur*O_4 tetragonal bipyramid that shares its equatorial vertices with four adjacent MoO_4 tetrahedra (Figs. 1a and 1b). The clusters are arranged in layers that are parallel to (001). The Rb^+ cations are located in the interlayer (Fig. 1d).

$Rb_6[(UO_2)_2O(MoO_4)_4]$. The structure contains chains of composition $[(UO_2)_2O(MoO_4)_4]^{6-}$ composed of *Ur*O_5 pentagonal bipyramids and MoO_4 tetrahedra (Figs. 2a and b). The chains involve dimers of *Ur*O_5 pentagonal bipyramids that share the O(6) vertex. The U(1)–O(6) and U(2)–O(6) bond lengths are 2.213(7) and 2.176(6) Å, which are considerably shorter than the typical $^{[7]}Ur$–O_{eq} bond length of 2.37 Å (24, 26). The chains are

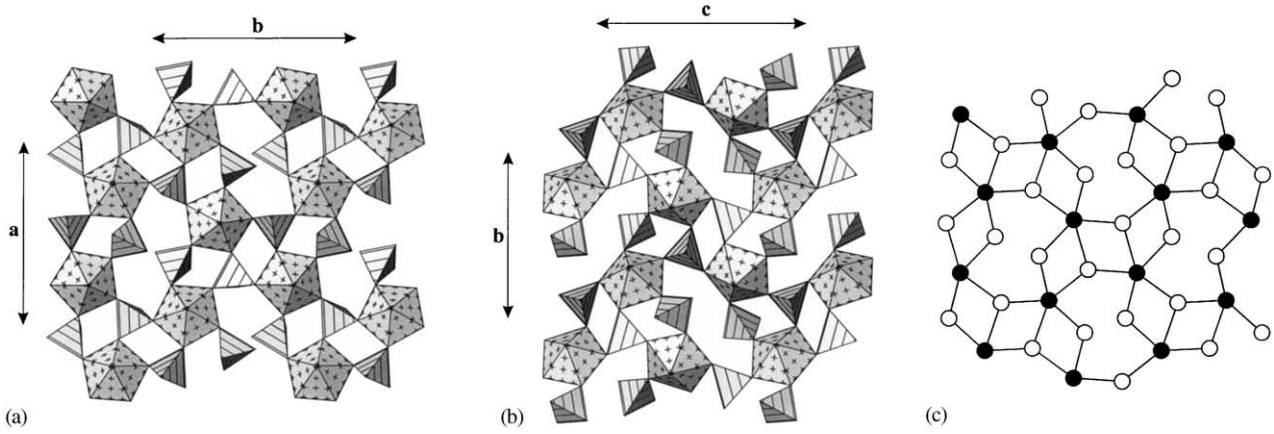

FIG. 4. Polyhedral representations of the $[(UO_2)(MoO_4)_2]^{2-}$ sheets in the structures of $Rb_2[(UO_2)(MoO_4)_2]$ (a) and $Rb_2[(UO_2)(MoO_4)_2](H_2O)$ (b), and (c) nodal representation of the $[(UO_2)(MoO_4)_2]^{2-}$ sheet (insets: U = black, Mo = white). Legend as in Fig. 1.

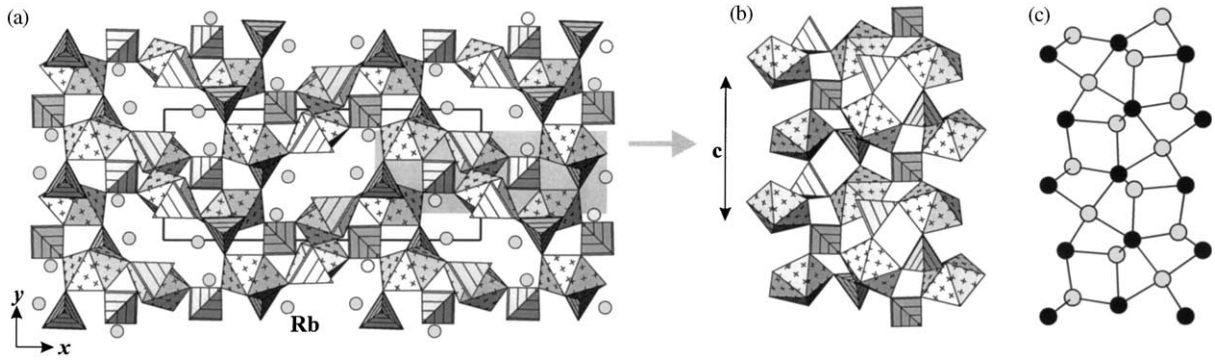

FIG. 6. (a) Polyhedral representation of the structure of $Rb_2[(UO_2)_2(MoO_4)_3]$ projected along [010], (b) its fundamental chain, and (c) its nodal representation (insets: U = black, Mo = white). Legend as in Fig. 1.

parallel to $[1\bar{1}0]$ and are arranged in layers that are parallel to (111) (Fig. 3). The Rb^+ cations provide linkage of the chains into a three-dimensional structure.

$Rb_2[(UO_2)(MoO_4)_2]$. The structure is based upon sheets of corner-sharing UrO_5 pentagonal bipyramids and MoO_4 tetrahedra (Fig. 4a). Within the sheets, the UrO_5 bipyramids are connected to five MoO_4 tetrahedra each, whereas there are two types of MoO_4 tetrahedra. The $Mo(3)O_4$ and $Mo(4)O_4$ tetrahedra are connected to three UrO_5 bipyramids each, whereas the $Mo(1)O_4$ and $Mo(2)O_4$ tetrahedra are connected to two UrO_5 bipyramids each.

TABLE 6
Atomic Coordinates and Displacement Parameters ($\times 10^4$ Å^2) for $Rb_2[(UO_2)(MoO_4)_2]$

	x	*y*	*z*	U_{eq}	U_{11}	U_{22}	U_{33}	U_{23}	U_{13}	U_{12}
U(1)	0.84403(3)	0.18155(3)	0.02867(3)	135(1)	1232(19)	117(2)	165(2)	−13(2)	130(14)	−0(1)
U(2)	0.33135(3)	0.32155(3)	−0.01240(3)	142(1)	1254(19)	125(2)	175(2)	−10(2)	111(15)	0(20)
Mo(1)	0.55375(9)	0.12542(8)	−0.07342(8)	192(2)	145(5)	184(6)	245(5)	−39(4)	1(4)	24(4)
Mo(2)	0.05485(9)	0.38517(9)	0.09374(8)	210(2)	183(5)	208(6)	244(6)	−62(5)	50(4)	−48(4)
Mo(3)	0.15048(8)	0.08936(8)	0.06056(8)	153(2)	132(4)	113(5)	215(5)	−6(4)	18(4)	1(4)
Mo(4)	0.64154(8)	0.40244(8)	−0.05044(8)	163(2)	133(4)	132(5)	222(5)	24(4)	15(4)	3(4)
Rb(1)	0.96477(12)	0.67458(11)	0.19370(10)	322(3)	389(8)	322(8)	252(7)	−46(6)	9(6)	50(7)
Rb(2)	0.73281(11)	0.95328(11)	0.18482(10)	303(3)	280(7)	359(8)	270(7)	−22(6)	30(5)	63(6)
Rb(3)	0.75633(13)	0.37887(12)	0.21375(10)	336(3)	402(8)	363(9)	248(7)	−74(6)	47(6)	44(7)
Rb(4)	0.45707(13)	0.15366(11)	0.21229(10)	334(3)	484(9)	280(8)	233(7)	−11(6)	7(6)	94(7)
O(1)	0.8294(7)	0.1734(6)	0.1648(6)	167(17)[a]						
O(2)	0.8624(7)	0.1897(7)	−0.1065(6)	210(19)[a]						
O(3)	0.3583(8)	0.3359(7)	0.1206(7)	280(20)[a]						
O(4)	0.3003(7)	0.3052(7)	−0.1455(7)	240(20)[a]						
O(5)	0.6829(7)	0.0961(7)	−0.0073(7)	270(20)	110(40)	180(50)	520(60)	10(50)	−30(40)	−40(40)
O(6)	0.4635(7)	0.1960(6)	−0.0058(7)	201(19)	190(40)	140(50)	280(50)	−60(40)	60(40)	50(30)
O(7)	0.5783(9)	0.1923(8)	−0.1776(8)	390(30)	360(60)	470(70)	350(60)	190(50)	60(50)	150(50)
O(8)	0.4899(8)	0.0180(8)	−0.1145(8)	350(30)	240(50)	260(60)	550(70)	−230(50)	−50(50)	−40(40)
O(9)	0.9212(7)	0.3333(7)	0.0645(7)	270(20)	150(40)	240(50)	420(60)	−50(40)	80(40)	−60(40)
O(10)	0.1503(7)	0.3549(7)	0.0035(6)	230(20)	150(40)	320(60)	220(40)	40(40)	40(40)	−10(40)
O(11)	0.1049(10)	0.3400(9)	0.2082(7)	470(30)	530(70)	650(90)	220(50)	20(60)	0(50)	−260(60)
O(12)	0.0449(10)	0.5102(8)	0.1099(10)	510(30)	560(80)	170(60)	820(90)	−210(60)	160(70)	−100(50)
O(13)	0.0311(7)	0.1587(7)	0.0776(7)	250(20)	100(40)	190(50)	470(60)	−30(40)	20(40)	40(30)
O(14)	0.2454(9)	0.1686(7)	0.0097(8)	340(30)	390(60)	40(40)	590(70)	−20(40)	140(50)	−20(40)
O(15)	0.8797(7)	0.0094(7)	0.0224(6)	196(18)	150(40)	160(50)	270(50)	−80(40)	−40(30)	40(30)
O(16)	0.2052(11)	0.0480(8)	0.1768(8)	470(30)	840(90)	210(60)	310(60)	10(50)	−230(60)	−80(60)
O(17)	0.6832(7)	0.5052(6)	0.0245(7)	240(20)	210(50)	100(40)	400(50)	0(40)	−90(40)	30(40)
O(18)	0.4985(7)	0.3910(7)	−0.0566(7)	250(20)	200(40)	190(50)	340(50)	−10(40)	20(40)	−30(40)
O(19)	0.7009(7)	0.2968(6)	0.0099(6)	195(18)	200(40)	90(40)	270(50)	0(30)	−60(40)	0(30)
O(20)	0.6784(9)	0.4171(8)	−0.1700(8)	410(30)	470(70)	440(70)	340(60)	140(50)	170(50)	50(60)

[a] Refined isotropically.

TABLE 7
Selected Bond Lengths (Å) in the Structure of $Rb_2[(UO_2)(MoO_4)_2]$

U(1)–O(2)	1.862(8)	Mo(3)–O(16)	1.75(1)	Rb(3)–O(16)*d*	2.76(1)
U(1)–O(1)	1.867(8)	Mo(3)–O(15)e	1.771(8)	Rb(3)–O(2)*j*	2.815(9)
U(1)–O(9)	2.311(9)	Mo(3)–O(14)	1.77(1)	Rb(3)–O(7)*j*	2.91(1)
U(1)–O(5)	2.315(8)	Mo(3)–O(13)	1.779(8)	Rb(3)–O(19)	2.995(9)
U(1)–O(19)	2.358(9)	⟨Mo(3)–O⟩	1.77	Rb(3)–O(1)	3.033(9)
U(1)–O(13)*a*	2.359(8)			Rb(3)–O(9)	3.045(9)
U(1)–O(15)	2.391(9)	Mo(4)–O(20)	1.73(1)	Rb(3)–O(17)	3.148(9)
⟨U(1)–O_{Ur}⟩	1.86	Mo(4)–O(18)	1.761(9)	⟨Rb(3)–O⟩	2.96
⟨U(1)–O_{eq}⟩	2.35	Mo(4)–O(17)	1.778(9)		
		Mo(4)–O(19)	1.780(8)	Rb(4)–O(8)*e*	2.79(1)
		⟨Mo(4)–O⟩	1.76	Rb(4)–O(4)*j*	2.893(9)
U(2)–O(3)	1.809(9)			Rb(4)–O(7)*j*	2.91(1)
U(2)–O(4)	1.819(9)	Rb(1)–O(12)*a*	2.73(1)	Rb(4)–O(3)	2.99(1)
U(2)–O(10)	2.302(8)	Rb(1)–O(11)*d*	2.79(1)	Rb(4)–O(6)	3.010(9)
U(2)–O(6)	2.357(8)	Rb(1)–O(10)*b*	2.934(9)	Rb(4)–O(18)*j*	3.178(9)
U(2)–O(14)	2.369(9)	Rb(1)–O(1)*f*	3.037(8)	Rb(4)–O(20)*j*	3.18(1)
U(2)–O(17)*b*	2.375(9)	Rb(1)–O(13)*d*	3.09(1)	Rb(4)–O(16)	3.41(1)
U(2)–O(18)	2.387(9)	Rb(1)–O(2)*g*	3.126(9)	⟨Rb(4)–O⟩	3.05
⟨U(2)–O_{Ur}⟩	1.80	Rb(1)–O(4)*b*	3.281(9)		
⟨U(2)–O_{eq}⟩	2.36	Rb(1)–O(16)*d*	3.32(1)		
		⟨Rb(1)–O⟩	3.04		
Mo(1)–O(7)	1.73(1)				
Mo(1)–O(8)	1.73(1)	Rb(2)–O(20)*h*	2.77(1)		
Mo(1)–O(6)	1.781(8)	Rb(2)–O(11)*d*	2.82(1)		
Mo(1)–O(5)	1.798(9)	Rb(2)–O(8)*b*	2.85(1)		
⟨Mo(1)–O⟩	1.76	Rb(2)–O(15)*i*	3.059(9)		
		Rb(2)–O(14)*b*	3.14(1)		
Mo(2)–O(12)	1.73(1)	Rb(2)–O(1)*i*	3.249(9)		
Mo(2)–O(11)	1.73(1)	Rb(2)–O(5)*i*	3.26(1)		
Mo(2)–O(9)*c*	1.802(9)	Rb(2)–O(3)*d*	3.35(1)		
Mo(2)–O(10)	1.812(9)	⟨Rb(2)–O⟩	3.06		
⟨Mo(2)–O⟩	1.77				

Note. $a = x+1, y, z$; $b = -x+1, -y+1, -z$; $c = x-1, y, z$; $d = -x+1, y+\frac{1}{2}, -z+\frac{1}{2}$; $e = -x+1, -y, -z$; $f = -x+2, y+\frac{1}{2}, -z+\frac{1}{2}$; $g = -x+2, -y+1, -z$; $h = x, -y+\frac{3}{2}, z+\frac{1}{2}$; $i = x, y+1, z$; $j = x, -y+\frac{1}{2}, z+\frac{1}{2}$.

The sheets of composition $[(UO_2)(MoO_4)_2]^{2-}$ are parallel to (001) and are linked by Rb^+ cations located in the interlayer (Fig. 5).

$Rb_2[(UO_2)_2(MoO_4)_3]$. The structure consists of a framework of corner-sharing UrO_5 bipyramids and MoO_4 tetrahedra with the composition $[(UO_2)_2(MoO_4)_3]^{2-}$ (Fig. 6a). The framework is composed of chains of polyhedra parallel to [001] (Fig. 6b). It contains channels parallel to [001] that are occupied by Rb^+ cations (Fig. 6a).

$Rb_2[(UO_2)_6(MoO_4)_7(H_2O)_2]$. The structure consists of a framework of corner-sharing UrO_5 pentagonal bipyramids, $UrO_4(H_2O)$ pentagonal bipyramids, and MoO_4 tetrahedra (Fig. 7). It is based upon double-thick sheets of UrO_5 pentagonal bipyramids and MoO_4 tetrahedra (Fig. 8a). Each sheet consists of two identical sheets of the type shown in Fig. 8b. The double sheets are parallel to (001) and are linked through $UrO_4(H_2O)$ pentagonal bipyramids. The Rb(1) atoms are located between the single sheets, within the double sheets, whereas the Rb(2) atoms are in the interlayer between adjacent double sheets.

DISCUSSION

Graphical Representation of Uranyl Molybdate Structural Units

The local structure of the uranyl molybdate units in Rb uranyl molybdates may be illustrated using a nodal representation. Each node corresponds to a $Ur\phi_n$ bipyramid ($\phi = O$, H_2O, $n = 4$ or 5) (black circle) or a MoO_4 tetrahedron (white circle). Nodes are connected if the polyhedra share at least one common vertex, and the number of connecting lines corresponds to the number of anions common to the polyhedra. Thus, each uranyl molybdate can be associated with a black-and-white graph that represents a topology of polyhedral linkage. The graphs for the uranyl molybdate units observed in the

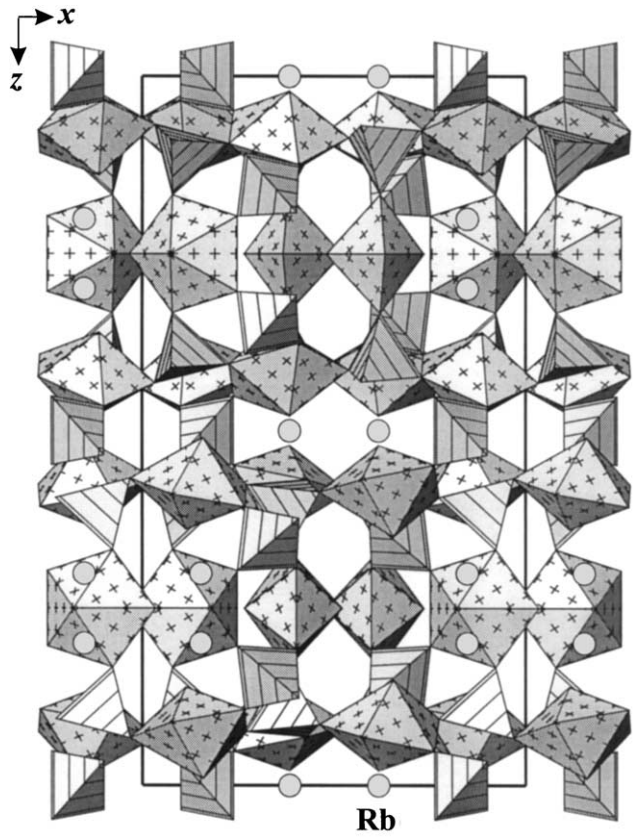

FIG. 7. Polyhedral representation of the structure of $Rb_2[(UO_2)_6(MoO_4)_7](H_2O)_2$ projected along [010].

structures of Rb uranyl molybdates are shown, for the $[(UO_2)(MoO_4)_4]^{6-}$ finite cluster in Fig. 1c, for the $[(UO_2)_2O(MoO_4)_4]^{6-}$ chain in Fig. 2c, for the $[(UO_2)(MoO_4)_2]^{2-}$ sheet in Fig. 4c, for the chain of the $[(UO_2)_2(MoO_4)_3]^{2-}$ framework in Fig. 6c, and for the single sheet of the $[(UO_2)_6(MoO_4)_7(H_2O)_2]^{2-}$ framework in Fig. 8c.

Relationships to the Structures of Other Alkali Metal Uranyl Molybdates

$Rb_6[(UO_2)(MoO_4)_4]$. The structure is related to that of $Cs_6[(UO_2)(MoO_4)_4]$, which was recently described in Ref. (19). The structure of $Cs_6[(UO_2)(MoO_4)_4]$ contains the finite cluster of composition $[(UO_2)(MoO_4)_4]^{6-}$ shown in Fig. 1a, but in the structure of $Cs_6[(UO_2)(MoO_4)_4]$, there are two symmetrically independent $[(UO_2)(MoO_4)_4]^{6-}$ clusters, one of which is centrosymmetric and the other which is non-centrosymmetric. In contrast, in $Rb_6[(UO_2)(MoO_4)_4]$ all clusters are centrosymmetric and symmetrically equivalent. In the structure of $Rb_6[(UO_2)(MoO_4)_4]$, all clusters are oriented in the same direction, and form layers, whereas, in the structure of $Cs_6[(UO_2)(MoO_4)_4]$, the clusters of two different types are oriented perpendicular to each other (19). This is reflected in the symmetry of the two structures; triclinic for $Cs_6[(UO_2)(MoO_4)_4]$ (space group $P\bar{1}$) and monoclinic for $Rb_6[(UO_2)(MoO_4)_4]$ (space group $C2/c$). It is interesting that the structure of $Na_6[(UO_2)(MoO_4)_4]$ is based on completely different

TABLE 8
Atomic Coordinates and Displacement Parameters ($\times 10^4$ Å^2) for $Rb_2[(UO_2)_2(MoO_4)_3]$

	x	y	z	U_{eq}	U_{11}	U_{22}	U_{33}	U_{23}	U_{13}	U_{12}
U(1)	0.782438(10)	0.78064(3)	0.59369(2)	134(1)	127(1)	142(1)	135(1)	290(9)	−6(90)	−0(80)
U(2)	0.524139(11)	0.17227(3)	0.67722(3)	152(1)	139(1)	154(1)	164(1)	74(9)	−8(100)	−20(80)
Mo(1)	0.53094(3)	0.25591(7)	0.06172(5)	164(1)	128(2)	169(3)	195(3)	135(19)	−13(2)	−2(190)
Mo(2)	0.63448(3)	0.98683(7)	0.37638(6)	160(1)	114(2)	210(3)	158(2)	711(19)	−0(190)	−7(2)
Mo(3)	0.69078(3)	0.42404(7)	0.73420(6)	184(1)	167(3)	186(3)	197(2)	49(2)	−8(2)	−49(2)
Rb(1)	0.64468(4)	0.80356(9)	0.93715(9)	368(2)	368(4)	260(4)	475(4)	19(3)	50(4)	36(3)
Rb(2)	0.60844(5)	0.51408(11)	0.39283(8)	414(2)	505(5)	444(5)	292(4)	−72(3)	−33(4)	214(4)
O(1)	0.6827(2)	0.8642(6)	0.4808(5)	309(12)	220(30)	420(30)	290(30)	210(20)	0(20)	30(20)
O(2)	0.6928(2)	0.6141(6)	0.6545(5)	259(11)	140(20)	300(30)	340(30)	180(20)	−81(19)	−64(18)
O(3)	0.5321(2)	0.0427(5)	0.0735(5)	278(11)	320(30)	180(20)	330(30)	40(20)	80(20)	−20(19)
O(4)	0.5823(3)	0.1074(7)	0.4737(5)	350(13)	280(30)	450(40)	320(30)	−20(20)	120(20)	40(20)
O(5)	0.7644(2)	0.9258(6)	0.7196(5)	257(10)	250(30)	260(30)	260(20)	−72(19)	−30(20)	50(20)
O(6)	0.5662(2)	0.0226(6)	0.7700(4)	262(11)	320(30)	210(30)	260(20)	1(19)	−70(20)	70(20)
O(7)	0.5201(3)	0.3136(6)	0.8871(4)	265(11)	380(30)	210(30)	210(20)	−10(19)	−90(20)	30(20)
O(8)	0.4650(2)	0.3260(6)	0.1525(6)	345(13)	220(30)	310(30)	500(40)	10(20)	60(20)	60(20)
O(9)	0.6879(2)	0.4565(6)	0.9165(4)	231(10)	250(30)	240(30)	200(20)	75(18)	−41(19)	50(20)
O(10)	0.6059(2)	0.3339(6)	0.1347(4)	203(10)	130(20)	280(30)	200(20)	−58(17)	−27(16)	−15(18)
O(11)	0.6190(2)	0.3277(6)	0.6730(6)	359(12)	280(30)	340(30)	450(30)	40(30)	−40(30)	−170(20)
O(12)	0.6850(2)	0.1129(6)	0.2790(5)	298(12)	300(30)	260(30)	330(30)	170(20)	110(20)	20(20)
O(13)	0.7583(3)	0.3180(6)	0.6861(6)	358(11)	340(30)	320(30)	410(30)	30(20)	120(30)	−10(20)
O(14)	0.4823(2)	0.3196(5)	0.5790(4)	248(10)	270(30)	230(30)	240(20)	70(20)	−90(20)	17(18)
O(15)	0.8029(3)	0.6292(6)	0.4726(5)	274(11)	360(30)	250(30)	220(20)	−90(20)	−20(20)	−30(20)
O(16)	0.5851(2)	0.8601(6)	0.2752(5)	313(12)	240(30)	350(30)	350(30)	−20(20)	−110(20)	−40(20)

TABLE 9
Selected Bond Lengths (Å) in the Structure of $Rb_2[(UO_2)_2(MoO_4)_3]$

U(1)–O(5)	1.766(4)	Mo(3)–O(13)	1.694(5)
U(1)–O(15)	1.781(5)	Mo(3)–O(11)	1.765(5)
U(1)–O(10)*a*	2.335(4)	Mo(3)–O(2)	1.772(4)
U(1)–O(9)*b*	2.347(4)	Mo(3)–O(9)	1.798(4)
U(1)–O(2)	2.362(4)	⟨Mo(3)–O⟩	1.757
U(1)–O(12)*a*	2.380(4)		
U(1)–O(1)	2.401(5)	Rb(1)–O(6)*f*	2.921(4)
⟨U(1)–O_{Ur}⟩	1.773	Rb(1)–O(15)*a*	2.946(5)
⟨U(1)–O_{eq}⟩	2.365	Rb(1)–O(9)	3.042(5)
		Rb(1)–O(14)*d*	3.092(5)
		Rb(1)–O(13)*a*	3.123(6)
U(2)–O(6)	1.764(4)	Rb(1)–O(3)*g*	3.309(5)
U(2)–O(14)	1.777(4)	Rb(1)–O(2)	3.325(5)
U(2)–O(11)	2.317(4)	Rb(1)–O(5)	3.376(5)
U(2)–O(3)*c*	2.357(5)		
U(2)–O(7)	2.365(4)	Rb(2)–O(10)	2.935(4)
U(2)–O(4)	2.368(5)	Rb(2)–O(7)*h*	2.973(5)
U(2)–O(16)*d*	2.420(5)	Rb(2)–O(11)	3.152(6)
⟨U(2)–O_{Ur}⟩	1.770	Rb(2)–O(16)	3.152(5)
⟨U(2)–O_{eq}⟩	2.365	Rb(2)–O(5)*i*	3.164(4)
		Rb(2)–O(2)	3.180(5)
Mo(1)–O(8)	1.704(5)	Rb(2)–O(8)*d*	3.225(5)
Mo(1)–O(7)*e*	1.782(4)	Rb(2)–O(1)	3.404(5)
Mo(1)–O(3)	1.789(5)		
Mo(1)–O(10)	1.797(4)		
⟨Mo(1)–O⟩	1.768		
Mo(2)–O(4)*f*	1.742(5)		
Mo(2)–O(1)	1.744(5)		
Mo(2)–O(12)*f*	1.749(5)		
Mo(2)–O(16)	1.760(5)		
⟨Mo(2)–O⟩	1.749		

Note. $a = -x+\frac{3}{2}, y+\frac{1}{2}, z+\frac{1}{2}$; $b = -x+\frac{3}{2}, y+\frac{1}{2}, z-\frac{1}{2}$; $c = -x+1, -y, z+\frac{1}{2}$; $d = -x+1, -y+1, z+\frac{1}{2}$; $e = x, y, z-1$; $f = x, y+1, z$; $g = x, y+1, z+1$; $h = -x+1, -y+1, z-\frac{1}{2}$; $i = -x+\frac{3}{2}, y-\frac{1}{2}, z-\frac{1}{2}$.

clusters of composition $[(UO_2)_2(MoO_4)_8]^{6-}$ that are formed by two UrO_5 pentagonal bipyramids and eight MoO_4 tetrahedra. Two of the MoO_4 tetrahedra bridge between two UrO_5 pentagonal bipyramids, whereas six others are terminal.

$Rb_6[(UO_2)_2O(MoO_4)_4]$. The $[(UO_2)_2O(MoO_4)_4]^{6-}$ chain observed in this structure (Figs. 2a and b) is closely related to chains recently found by the authors in the structures of $Na_6[(UO_2)_2O(MoO_4)_4]$ and $K_6[(UO_2)_2O(MoO_4)_4]$ (18). The uranyl molybdate chains in these structures are topologically identical to that in $Rb_6[(UO_2)_2O(MoO_4)_4]$, but they are different from a geometrical point of view. Figures 2b and 2d compare the $[(UO_2)_2O(MoO_4)_4]^{6-}$ chains in the structures of $Rb_6[(UO_2)_2O(MoO_4)_4]$ and $Na_6[(UO_2)_2O(MoO_4)_4]$, respectively. Note that the chain is straight in $Rb_6[(UO_2)_2O(MoO_4)_4]$ and that it is slightly corrugated in $Na_6[(UO_2)_2O(MoO_4)_4]$. In addition, the orientation of the MoO_4 tetrahedra on the edges of the chains differs in the two structures. In $Rb_6[(UO_2)_2O(MoO_4)_4]$, the MoO_4 tetrahedra along both edges of the chain are in the same orientation, whereas in $Na_6[(UO_2)_2O(MoO_4)_4]$ they are in opposite orientations on either side of the chain. The geometrical differences of the $[(UO_2)_2O(MoO_4)_4]^{6-}$ chains depicted in Figs. 2b and 2d are due to the presence of different alkali metal cations in the structures. This conformation becomes possible owing to the highly flexible nature of the U–O–Mo linkages, as demonstrated in several recent studies (17–21).

$Rb_2[(UO_2)(MoO_4)_2]$. This compound is isostructural with $K_2[(UO_2)(MoO_4)_2]$, which was described by Sadikov *et al.* (11). The $[(UO_2)(MoO_4)_2]^{2-}$ sheet has the same topology as the sheet in the structures of $M_2[(UO_2)(MoO_4)_2](H_2O)$ ($M = NH_4^+$ (28), K^+ (17), Rb^+ (16), Cs^+ (15)). A similar topology was recently observed for a $[(UO_2)(SeO_3)_2]$ sheet in uranyl selenites (29). However, the $[(UO_2)(MoO_4)_2]^{2-}$ sheet in the structure of $Na_2[(UO_2)(MoO_4)_2]$ is topologically different (17). Figures 4a and 4b compare the geometries of the $[(UO_2)(MoO_4)_2]^{2-}$ sheets in the structures of $Rb_2[(UO_2)(MoO_4)_2]$ (this work) and

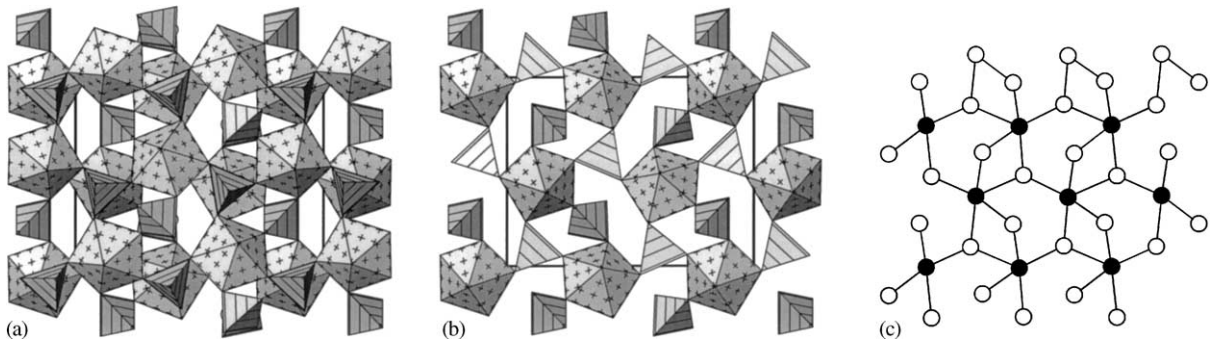

FIG. 8. (a) Polyhedral representation of the double uranyl molybdate sheet in the structure of $Rb_2[(UO_2)_6(MoO_4)_7](H_2O)_2$, (b) one of its two components, and (c) its nodal representation (insets: U = black, Mo = white). Legend as in Fig. 1.

TABLE 10
Atomic Coordinates and Displacement Parameters ($\times 10^4$ Å^2) for $Rb_2[(UO_2)_6(MoO_4)_7(H_2O)_2]$

	x	y	z	U_{eq}	U_{11}	U_{22}	U_{33}	U_{23}	U_{13}	U_{12}
U(1)	0.13340(6)	0.09493(7)	$\frac{1}{4}$	169(2)	194(4)	176(4)	137(3)	0	0	−52(3)
U(2)	−0.36915(4)	−0.56922(5)	0.416037(18)	117(1)	117(2)	99(2)	136(2)	0(2)	−10(2)	40(19)
U(3)	−0.13499(4)	−0.05959(5)	0.427042(19)	131(1)	122(2)	121(2)	148(2)	13(2)	6(2)	−113(19)
U(4)	−0.39554(6)	−0.98419(7)	$\frac{1}{4}$	139(2)	183(4)	126(3)	107(3)	0	0	8(3)
Mo(1)	−0.17089(13)	$\frac{1}{4}$	$\frac{1}{2}$	154(3)	110(8)	119(8)	232(9)	30(7)	0	0
Mo(2)	−0.39149(8)	−0.91336(10)	0.40221(4)	121(2)	135(6)	100(5)	128(5)	−13(4)	12(4)	−22(4)
Mo(3)	−0.33543(9)	−0.25969(11)	0.34626(4)	128(2)	151(6)	114(5)	118(5)	8(4)	10(5)	8(4)
Mo(4)	0.10611(9)	0.08109(11)	0.40020(5)	149(2)	129(6)	148(6)	170(5)	19(4)	19(5)	−16(5)
Rb(1)	−0.3841(2)	$-\frac{1}{4}$	$\frac{1}{2}$	329(6)	520(17)	195(11)	273(11)	−54(8)	0	0
Rb(2)[a]	0.1520(4)	−0.2858(4)	0.2006(2)	752(16)	760(40)	410(30)	1080(40)	−300(30)	−150(30)	0(20)
O(1)	−0.2653(10)	0.0018(14)	$\frac{1}{4}$	210(30)	200(80)	260(90)	190(70)	0	0	0(60)
O(2)	−0.4287(7)	−0.7745(8)	0.4314(4)	150(20)	190(50)	90(50)	190(50)	10(40)	−30(40)	−10(40)
O(3)	−0.1135(7)	−0.0114(10)	0.3610(3)	200(20)	230(60)	250(50)	130(40)	40(40)	30(40)	−10(40)
O(4)	−0.3838(7)	−0.5095(9)	0.4794(4)	230(20)	270(60)	210(50)	200(50)	−50(40)	−80(50)	−30(50)
O(5)	−0.1578(8)	−0.1115(10)	0.4906(4)	250(20)	260(60)	250(60)	240(60)	70(50)	80(50)	−100(50)
O(6)	−0.5212(11)	−0.9699(14)	$\frac{1}{4}$	250(30)	250(90)	210(80)	300(80)	0	0	−30(70)
O(7)	−0.3446(8)	−0.6260(9)	0.3510(4)	260(30)	440(70)	130(50)	210(50)	−70(40)	20(50)	−60(50)
O(8)	−0.2711(7)	−0.9393(9)	0.4241(4)	200(20)	130(50)	170(50)	310(60)	0(40)	50(40)	10(40)
O(9)	−0.1002(8)	0.1379(9)	0.4655(4)	220(20)	180(50)	190(50)	280(60)	−20(40)	−90(50)	−20(40)
O(10)	−0.4018(8)	−0.1539(9)	0.3084(3)	210(20)	290(60)	240(60)	110(40)	50(40)	−30(50)	50(50)
O(11)	0.2257(7)	0.0545(9)	0.4059(4)	210(20)	140(50)	260(60)	240(50)	−30(40)	100(40)	40(40)
O(12)	−0.3797(8)	−0.8962(10)	0.3339(4)	270(30)	480(80)	230(60)	110(50)	−30(40)	50(50)	0(50)
O(13)	0.0755(8)	0.2377(9)	0.4110(4)	260(30)	200(60)	130(50)	450(70)	60(50)	20(50)	−30(40)
O(14)	−0.2670(7)	−0.1795(9)	0.3927(4)	230(20)	220(60)	170(50)	300(60)	−10(50)	−80(50)	−60(40)
O(15)	−0.2477(9)	−0.3286(11)	0.3034(4)	300(30)	420(80)	270(70)	210(60)	20(50)	40(50)	130(50)
O(16)	−0.4617(7)	−0.0462(8)	0.4140(4)	160(20)	210(50)	90(50)	180(50)	30(40)	−40(40)	20(40)
O(17)	−0.4080(7)	−0.3708(9)	0.3767(4)	180(20)	150(50)	160(50)	240(50)	120(40)	0(40)	0(40)
O(18)	−0.2373(8)	0.1758(10)	0.5484(4)	250(30)	270(60)	150(50)	350(60)	30(50)	120(50)	−40(40)
O(19)	−0.0338(12)	0.0062(17)	$\frac{1}{4}$	380(50)	320(100)	470(120)	360(100)	0	0	−260(90)
O(20)	0.0322(7)	−0.0272(9)	0.4329(4)	160(20)	120(50)	190(50)	170(50)	20(40)	−10(40)	0(40)
O(21)	−0.3670(14)	−0.7493(13)	$\frac{1}{4}$	380(50)	800(150)	130(80)	220(80)	0	0	−20(90)
O(22)	0.0781(9)	0.0571(12)	0.3331(4)	400(30)	350(70)	670(100)	170(60)	−10(50)	60(50)	−260(70)
O(23)	0.0728(13)	0.2421(15)	$\frac{1}{4}$	370(40)	470(120)	220(90)	440(100)	0	0	−90(80)
O(24)	0.1805(14)	−0.0538(14)	$\frac{1}{4}$	420(50)	610(130)	150(90)	490(110)	0	0	40(80)

[a] s.o.f. = 0.50.

$Rb_2[(UO_2)(MoO_4)_2(H_2O)]$ (16), respectively. The sheet in $Rb_2[(UO_2)(MoO_4)_2(H_2O)]$ is distorted relative to that observed in $Rb_2[(UO_2)(MoO_4)_2]$. This again reflects the flexible nature of the U–O–Mo linkages.

$Rb_2[(UO_2)_2(MoO_4)_3]$. This compound is isostructural with α-$Cs_2[(UO_2)_2(MoO_4)_3]$ (21). The unit-cell parameters for α-$Cs_2[(UO_2)_2(MoO_4)_3]$ [$a-b-c$ (Å): 20.430–8.555–9.855] are larger than those for its Rb analogue [20.214–8.374–9.745], due to the larger ionic radius of the Cs^+ cation (1.74 Å) in comparison to that of Rb^+ (1.61 Å, radii are taken from (30) for eightfold coordination). It is interesting that α-$Cs_2[(UO_2)_2(MoO_4)_3]$ was prepared by hydrothermal methods, whereas solid-state reactions invariably produce crystals of β-$Cs_2[(UO_2)_2(MoO_4)_3]$ that has a layered structure (21). A phase isostructural with β-$Cs_2[(UO_2)_2(MoO_4)_3]$ has not yet been observed for the composition $Rb_2(UO_2)_2(MoO_4)_3$.

$Rb_2[(UO_2)_6(MoO_4)_7(H_2O)_2]$. This compound is isostructural with $M_2[(UO_2)_6(MoO_4)_7(H_2O)_2]$ ($M = Cs^+$, NH_4^+) (20). However, the unit-cell parameters for the Rb compound [$a-b-c$ (Å): 13.961–10.752–25.579] are approximately the same as those for Cs compound [13.990–10.808–25.671] and the NH_4 compound [13.970–10.747–25.607]. This is an indication that the $[(UO_2)_6(MoO_4)_7(H_2O)_2]^{2-}$ framework may accommodate cations of different size without significant change of its geometric parameters. This suggests that the cations can be replaced during ion-exchange reaction, but an experimental verification of this hypothesis is necessary.

CONCLUSIONS

The Rb uranyl molybdates described herein further demonstrate the structural complexity and variability of uranyl molybdates. The sharing of only vertices between

TABLE 11
Selected Bond Lengths (Å) in the Structure of $Rb_2[(UO_2)_6(MoO_4)_7(H_2O)_2]$

U(1)–O(23)	1.73(2)	Mo(2)–O(12)	1.748(9)
U(1)–O(24)	1.79(2)	Mo(2)–O(16)*h*	1.759(9)
U(1)–O(22),*a*	2.26(1) 2 ×	Mo(2)–O(8)	1.764(9)
U(1)–O(15)*b*,*c*	2.30(1) 2 ×	Mo(2)–O(2)	1.79(1)
U(1)-H_2O(19)	2.52(2)	⟨Mo(2)–O⟩	1.77
⟨U(1)–O_{Ur}⟩	1.76		
⟨U(1)-ϕ_{eq}⟩	2.33	Mo(3)–O(15)	1.749(9)
		Mo(3)–O(10)	1.75(1)
U(2)–O(4)	1.756(9)	Mo(3)–O(14)	1.76(1)
U(2)–O(7)	1.81(1)	Mo(3)–O(17)	1.80(1)
U(2)–O(18)*d*	2.35(1)	⟨Mo(3)–O⟩	1.77
U(2)–O(2)	2.38(1)		
U(2)–O(11)*e*	2.391(9)	Mo(4)–O(11)	1.70(1)
U(2)–O(16)*f*	2.42(1)	Mo(4)–O(22)	1.76(1)
U(2)–O(17)	2.421(9)	Mo(4)–O(20)	1.766(9)
⟨U(2)–O_{Ur}⟩	1.78	Mo(4)–O(13)	1.78(1)
⟨U(2)-ϕ_{eq}⟩	2.39	⟨Mo(4)–O⟩	1.75
U(3)–O(3)	1.75(1)	Rb(1)–O(4),*d*	2.84(1)
U(3)–O(5)	1.791(9)	Rb(1)–O(2)*k*, *l*	3.16(1)
U(3)–O(8)*g*	2.30(1)	Rb(1)–O(14),*d*	3.28(1)
U(3)–O(13)*e*	2.364(9)	Rb(1)–O(16),*d*	3.288(9)
U(3)–O(20)	2.37(1)	Rb(1)–O(17),*d*	3.43(1)
U(3)–O(9)	2.39(1)	Rb(1)–O(5),*d*	3.50(1)
U(3)–O(14)	2.42(1)	⟨Rb(1)–O⟩	3.25
⟨U(3)–O_{Ur}⟩	1.77		
⟨U(3)-ϕ_{eq}⟩	2.37	Rb(2)–O(24)*m*	2.82(1)
		Rb(2)–O(3)*h*	2.94(1)
U(4)–O(1)*h*	1.76(2)	Rb(2)–O(19)*h*	3.05(2)
U(4)–O(6)	1.82(1)	Rb(2)–O(7)	3.05(2)
U(4)–O(12),*a*	2.356(9)	Rb(2)–O(1)*h*	3.28(2)
U(4)–O(10)*h*,*i*	2.359(9)	Rb(2)–O(23)*h*	3.40(2)
U(4)-H_2O(21)	2.56(2)	Rb(2)–O(21)	3.45(1)
⟨U(4)–O_{Ur}⟩	1.79	Rb(2)–O(12)	3.51(1)
⟨U(4)-ϕ_{eq}⟩	2.40	⟨Rb(2)–O⟩	3.19
Mo(1)–O(9),*j*	1.74(1) 2 ×		
Mo(1)–O(18),*j*	1.79(1) 2 ×		
⟨Mo(1)–O⟩	1.77		

Note. $a = x, y, -z+\frac{1}{2}$; $b = -x, y+\frac{1}{2}, z$; $c = -x, y+\frac{1}{2}, -z+\frac{1}{2}$; $d = x, -y-\frac{1}{2}, -z+1$; $e = -x, y-\frac{1}{2}, z$; $f = -x-1, y-\frac{1}{2}, z$; $g = x, y+1, z$; $h = x, y-1, z$; $i = x, y-1, -z+\frac{1}{2}$; $j = x, -y+\frac{1}{2}, -z+1$; $k = -x-1, y+\frac{1}{2}, z$; $l = -x-1, -y-1, -z+1$; $m = -x, y-\frac{1}{2}, -z+\frac{1}{2}$.

uranyl polyhedra and MoO_4 tetrahedra results in a considerable flexibility of the uranyl molybdate units, owing to the flexibility of the U–O–Mo linkages. Rb uranyl molybdates can adopt each of the structure types described for uranyl minerals and inorganic compounds (24, 25): finite clusters, chains, sheets and frameworks of polyhedra of higher bond valence. The size of the alkali metal cation influences the topology and geometry of the uranyl molybdate units. Sometimes, the observed changes are dramatic (topologically different $[(UO_2)(MoO_4)_4]^{6-}$ units in the structures of $Na_6[(UO_2)(MoO_4)_4]$ and $M_2[(UO_2)(MoO_4)_4]$ (M = Rb, Cs)). In other cases, the changes involve relative rotations of polyhedra that result in geometrically different structures. Thus, many new topologies and geometrical variations are possible for uranyl molybdates, and these will be the subjects of forthcoming papers.

ACKNOWLEDGMENTS

This research was supported by the Environmental Management Sciences Program of the United States Department of Energy (Grant DE-FG07-97ER 14820) and by the Russian Foundation for Basic Research (S.V.K., Grant 01-05-64883).

REFERENCES

1. R. J. Finch and T. Murakami, *Rev. Mineral.* **38,** 91 (1999).
2. E. C. Buck, D. J. Wronkiewicz, P. A. Finn, and J. K. Bates, *J. Nucl. Mater.* **249,** 70 (1997).
3. C. Dion, A. Noël, and J. Laureyns, *Bull. Soc. Chim. Fr.* **1977**(I), 1115–1120 (1977).
4. C. Dion and A. Noël, *Bull. Soc. Chim. Fr.* **1981**(I), 185 (1981).
5. C. Dion and A. Noël, *Bull. Soc. Chim. Fr.* **1981**(I), 371 (1981).
6. C. Dion and A. Noël, *Bull. Soc. Chim. Fr.* **1981**(I), 413 (1981).
7. C. Dion and A. Noël, *Bull. Soc. Chim. Fr.* **1982**(I), 188 (1982).
8. T. I. Krasovskaya, Yu. A. Polyakov, and I. A. Rozanov, *Izv. Akad Nauk SSSR, Neorg. Mater.* **17,** 695 (1981).
9. C. Dion and A. Noël, *Bull. Soc. Chim. Fr.* **1983**(I), 257 (1983).
10. C. Dion and A. Noël, *Bull. Soc. Chim. Fr.* **1985**(I), 735 (1985).
11. G. G. Sadikov, T. I. Krasovskaya, Yu. A. Polyakov, and V. P. Nikolaev, *Izv. Akad Nauk SSSR, Neorg. Mater.* **24,** 109 (1988).
12. T. I. Krasovskaya, Yu. A. Polyakov, and I. A. Rozanov, *Izv. Akad Nauk SSSR, Neorg. Mater.* **16,** 1824 (1980).
13. V. N. Serezhkin, E. E. Tatarinova, and L. B. Serezhkina, *Zh. Neorg. Khim.* **32,** 227 (1987).
14. N. L. Misra, K. L. Chawla, V. Venugopal, N. C. Jayadevan, and D. D. Sood, *J. Nucl. Mater.* **226,** 120 (1995).
15. R. K. Rastsvetaeva, A. V. Barinova, A. M. Fedoseev, N. A. Budantseva, and Yu. V. Nekrasov, *Dokl. Akad. Nauk* **365,** 68 (1999).

TABLE 12
Bond-Valence Analyses (v.u.) for Rubidium Uranyl Molybdates

	$Rb_6[(UO_2)(MoO_4)_4]$	$Rb_6[(UO_2)_2O(MoO_4)_4]$	$Rb_2[(UO_2)(MoO_4)_2]$	$Rb_2[(UO_2)_2(MoO_4)_3]$	$Rb_2[(UO_2)_6(MoO_4)_7(H_2O)_2]$
Rb	1.14, 1.28, 1.00, 0.99	1.00, 1.21, 0.99, 0.99, 0.97, 1.11	1.13, 1.07, 1.12, 1.06	0.83, 0.78	1.00, 0.80
U	6.12	5.98, 6.03	5.62, 5.85	6.09, 6.09	6.43, 5.90, 6.10, 5.82
Mo	5.94, 5.85	5.89, 5.91, 5.79, 6.00	5.97, 5.84, 5.83, 5.92	5.86, 6.13, 6.06	5.82, 5.88, 5.86, 5.86
O	1.89–2.15	1.61, 1.78–2.16	1.73–2.09	1.80–2.15	1.66–2.23
H_2O	—	—	—	—	0.51–0.61

16. V. N. Khrustalev, G. B. Andreev, M. Yu. Antipin, A. M. Fedoseev, N. A. Budantseva, and I. B. Shirokova, *Zh. Neorg. Khim.* **45,** 1996 (2000).
17. S. V. Krivovichev, R. J. Finch, and P. C. Burns, *Can. Mineral.* **40,** 193–200 (2002).
18. S. V. Krivovichev and P. C. Burns, *Can. Mineral.* **39,** 197 (2001).
19. S. V. Krivovichev and P. C. Burns, *Can. Mineral.* **40,** 201–209 (2002).
20. S. V. Krivovichev and P. C. Burns. *Can. Mineral.* **39,** 207 (2001).
21. S. V. Krivovichev, C. L. Cahill, and P. C. Burns, *Inorg. Chem.* **41,** 34 (2002).
22. E. E. Tatarinova, L. B. Serezhkina, and V. N. Serezhkin, *Radiokhimiya* **3,** 61 (1991).
23. J. A. Ibers and W. C. Hamilton, Eds., *International Tables for X-Ray Crystallography*, Vol. IV. The Kynoch Press, Birmingham, UK, 1974.
24. P. C. Burns, *Rev. Mineral.* **38,** 23 (1999).
25. P. C. Burns, M. L. Miller, and R. C. Ewing, *Can. Mineral.* **34,** 845 (1996).
26. P. C. Burns, F. C. Hawthorne, and R. C. Ewing, *Can. Mineral.* **35,** 1551 (1997).
27. N. E. Brese and M. O'Keeffe, *Acta Crystallogr. B* **47,** 192 (1991).
28. G. B. Andreev, M. Yu. Antipin, A. M. Fedoseev, and N. A. Budantseva, *Koord. Khim.* **27,** 227 (2001).
29. P. M. Almond and T. E. Albrecht-Schmitt, *Inorg. Chem.* **41,** 1177 (2002).
30. R. D. Shannon, *Acta Crystallogr. A* **32,** 751 (1976).